SF2A 2009
M. Heydari-Malayeri, C. Reylé and R. Samadi (eds)

THERMOHALINE INSTABILITY AND ROTATION-INDUCED MIXING IN LOW AND INTERMEDIATE-MASS STARS.

Lagarde, N.[1] and Charbonnel, C.[1,2]

Abstract. The classical theory of stellar evolution predicts that low-mass stars are strong producers of ^3He, in contradiction with abundance observations of this element in Galactic HII regions and in the protosolar nebula. However in 2007, Charbonnel & Zahn showed that thermohaline mixing drastically reduces the yields of ^3He producted by low-mass red giants. Simultaneously this mechanism changes the surface of carbon isotopic ratio as well as the abundances of lithium, carbon and nitrogen. In this paper, we present and discuss models computed with the code STAREVOL that include the transport of chemical species in the radiative regions due to thermohaline instability and to rotational mixing. We compare our theorical predictions with recent observations.

1 Introduction

During the first dredge-up, the standard theory predicts that the convective envelope deepens in mass, and engulfes hydrogen-processed material. This induces a decrease of the surface $^{12}C/^{13}C$, Li, or ^{12}C abundances, while ^{14}N and ^3He abundances increase. After the first dredge-up, the convective envelope retracts and the hydrogen burning shell moves outward (in mass). The standard theory predicts ^3He is present and does not change further. The observations in open clusters and in galactic field are agree with standard theory at the first dredge-up. However, a second change in the surface abundance is observed latter, on RGB, more precisely at the BUMP luminosity. Eggleton et al. (2006) have proposed that the inversion of molecular weight created by $^3He(^3He, 2p)^4He$ reaction may be at the origin of mixing on the red giant branch, for low-mass stars. Charbonnel & Zahn showed that this inversion sets of the so-called thermohaline mixing. Which is a double diffusive instability. In following sections, we present some results obtained with the code STAREVOL, including thermohaline mixing and rotation-induced mixing, at solar metallicity.

2 Models and results

We discuss in this section the effects of rotation-induced mixing and thermohaline mixing in a low-mass star ($M = 1.25M_\odot$) and in a intermediate-mass star ($M = 2.0M_\odot$).

2.1 Low-mass star, $M = 1.25M_\odot$

In figure 1, we present a Kippenhahn diagram for a $M = 1.25M_\odot$ star, with thermohaline mixing and rotation with $V_{ZAMS} = 110km/s$. We note that the thermohaline zone (blue) extends between the convective envelope (CE, in black hatching) and the external wing of the hydrogen burning shell (HBS) at the luminosity near the BUMP luminosity. In figure 1, we present also the evolution of surface carbon isotopic ratio for the same star. Due to thermohaline mixing, $^{12}C/^{13}C$ decreases at the BUMP luminosity contrary to the standard theory. We note that the value after the first dredge-up is lower with rotation. Due to rotation-induced mixing on the main sequence (see Palacios, A. et al. 2003, 2006). We note that the luminosity where thermohaline mixing connect the CE and HBS is the same in both cases. In addition, the value of $^{12}C/^{13}C$ at the end of RGB is also very similar in all cases.

[1] Geneva Observatory, 51 chemin des Mailettes, 1290 Sauverny, Switzerland
[2] LATT, CNRS UMR 5572, Universite de Toulouse, 14 avenue Edouard Belin, F-31400 Toulouse Cedex 04, France

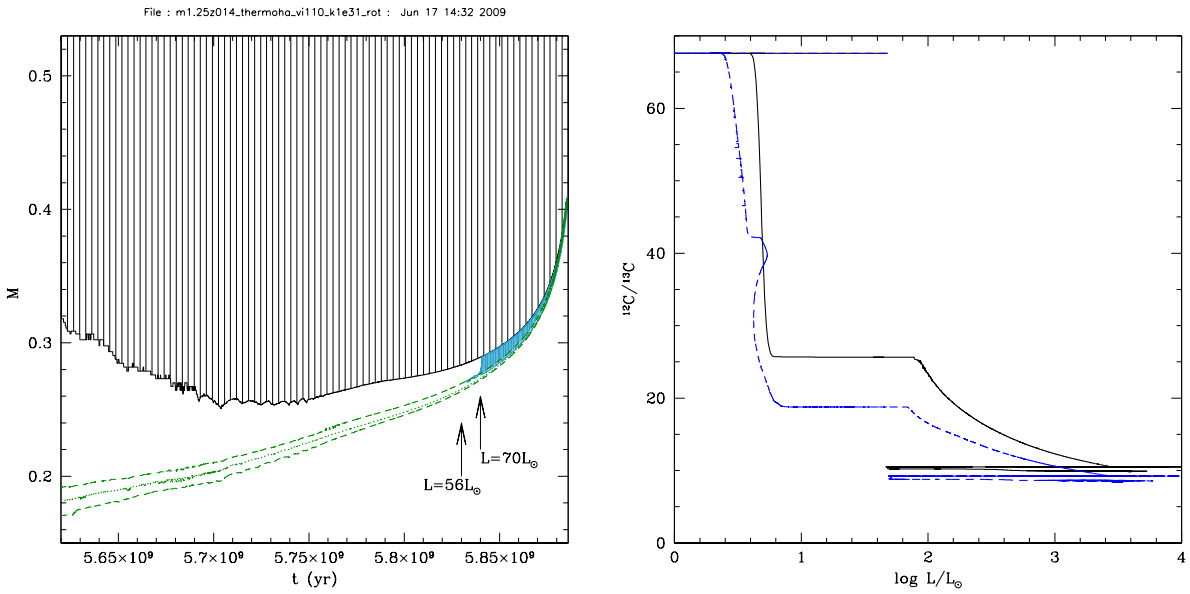

Fig. 1. Left : Kippenhahn diagram for a $M = 1.25M\odot$, $Z_\odot$ star, computed with thermohaline mixing and rotation-induced mixing ($V_{ZAMS} = 110km/s$). Thermohaline zone (between HBS and CE) is shown as blue hatching zone. **Right**: The evolution of surface carbon isotopic ratio as a function of luminosity. The solid line represents the standard model, and the dashed line represents the model computed with rotation $V_{ZAMS} = 110km/s$. Thermohaline mixing is present in both cases.

2.2 Intermediate-mass star : $M = 2.0M_\odot$

In figure 2, we present a Kippenhahn diagram for $M = 2.0M_\odot$, $Z_\odot$ star, with and without rotation. When the rotation is not included (left pannel), the thermohaline zone connects the CE with HBS at the end of RGB. So, it has not an effect on the surface abundance, as shown in figure 3. However, when the rotation is included (right pannel, fig 2), the thermohaline zone connects CE and HBS earlier in luminosity than in the model without rotation. In fact, the rotation changes the stellar structure on the main sequence, and favors the thermohaline mixing, in intermediate-mass stars. So, the evolution of $^{12}C/^{13}C$ for this star changes on the RGB. As can be seen in fig 3, the value of $^{12}C/^{13}C$ after the first drege-up decreases when the initial rotation velocity increases. Otherwise, the value of $^{12}C/^{13}C$ at the end of RGB decreases when the initial velocity increases. So the rotation favors the effect of thermohaline mixing on the RGB in the intermediate-mass star.

2.3 Comparison with observations

We compare our predictions with the observations in M67 by Gilroy & Brown (1991), and in 10 open clusters by Smiljanic et al. (2008) (see Smiljanic et al. 2009 (in press) for other comparisons). The standard theory does not explain the lower value of $^{12}C/^{13}C$ observed in the open clusters. For low-mass stars ($M \leq 1.7M_\odot$), thermohaline mixing explains well the observed carbon isotopic ratio, and the value of $^{12}C/^{13}C$ with rotation is approximatly the same, as discussed above. However, for interdiate-mass stars ($M \geq 1.7M_\odot$), rotation-induced mixing favors the effect of thermoaline mixing on the RGB.

3 Conclusion

An inversion of molecular weight created by the $^3He(^3He, 2p)^4He$ reaction is at the origin of thermohaline mixing in RGB stars brighter than the BUMP luminosity. This mixing connects the convective envelope with the external wing of hydrogen burning shell and induces surface abundance modifications. The introduction of this process in models of rotating stars allows us to explain the carbon isotopic ratio anomalies in giant stars

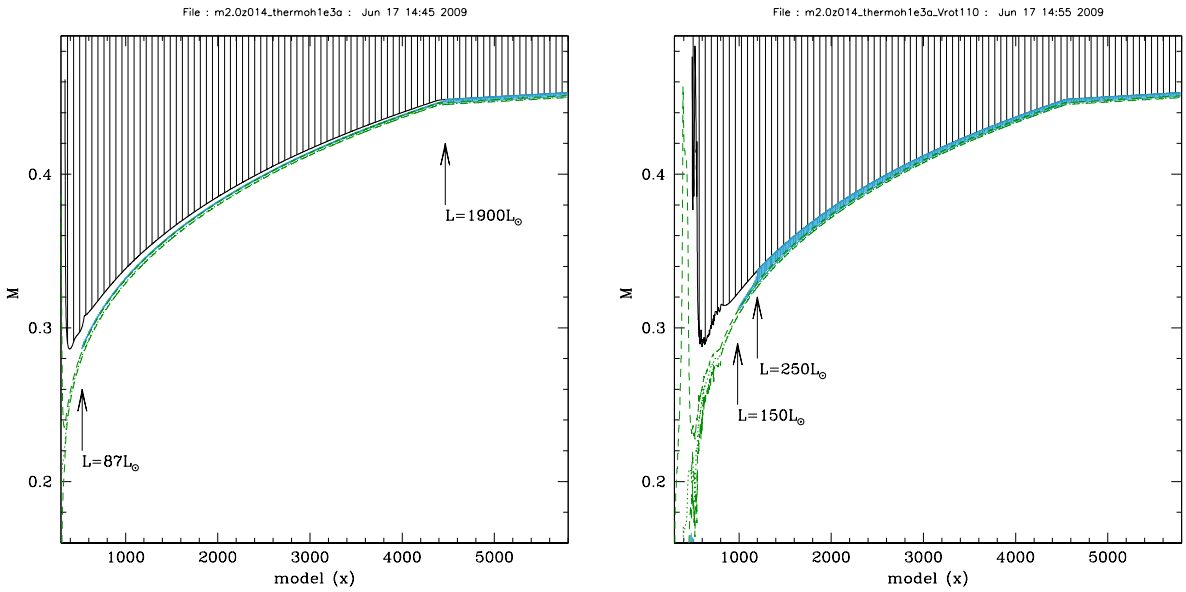

Fig. 2. Kippenhahn diagram for $M = 2.0M_{\odot}$, $Z_{\odot}$ star computed without rotation (**Left**), and with rotation (**Right**). In both cases, thermohaline mixing is included, and the region where it developsis represented with blue hatching between CE (black hachting) and HBS (green zone). The luminosity of BUMP and the luminosity when the thermohaline mixing connects CE and HBS are indicated.

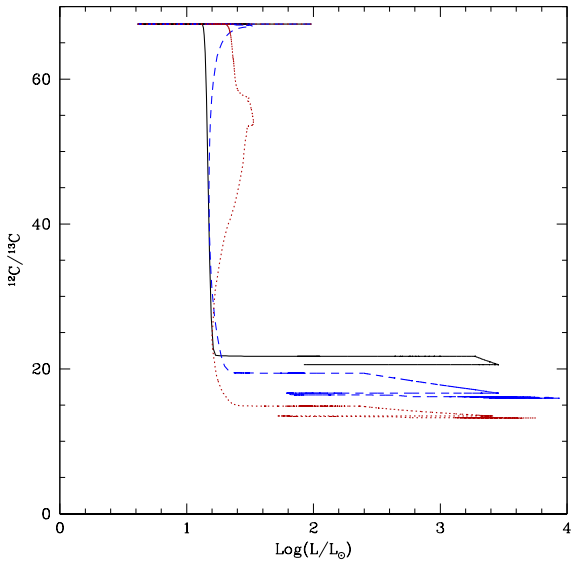

Fig. 3. The evolution of surface carbon isotopic ratio as a function of luminosity for a $M = 2.0M_{\odot}$, $Z_{\odot}$ star. Thermohaline mixing is present in all cases. The solid line is for the model without rotation, the dashed line for the model with $V_{ZAMS} = 110km/s$, and the dotted line for the model with $V_{ZAMS} = 180km/s$.

of open clusters over a broad range of turn-off.

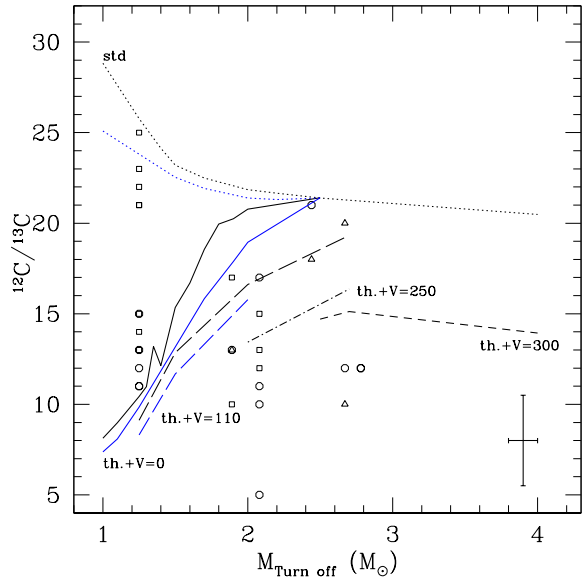

Fig. 4. Theorical predictions compared with observations of the carbon isotopic ratio, $^{12}C/^{13}C$, as a function of the open cluster turn-off mass. Our theorical values of $^{12}C/^{13}C$ as a function of the initial stellar mass : the standard models is shown as dotted lines ; the thermohaline models is shown as a solid line ; and the rotational models are shown as a long dashed lines for $V_{ZAMS} = 110km/s$; as a dot-dashed lines for $V_{ZAMS} = 250km/s$; and as a short dashed lines for $V_{ZAMS} = 300km/s$. For all theoricals models, values at the tip-RGB are shown in black and values at the tip-AGB are shown in blue. Observations of $^{12}C/^{13}C$ in open cluster by Smiljanic et al. (2008) and Gilroy & Brown (1991) : possible RGB stars are shown as open square, clump giants as open triangle, and possible early-AGB as open circle. For observations a typical error bar is shown.

References

Charbonnel, C., & Zahn, J.P., 2007, A&A, 467, L15-L18.

Eggleton, P.P., Dearborn, D.S.P., Lattanzio, J.C., 2006, Science, 314, 1580

Gilroy, K.K., Brown, J.A., 1991, ApJ, 371, 578-583

Palacios, A., Talon, S., Charbonnel, C., Forestini, M., 2003, A&A, 399, 603-616

Palacios, A., Charbonnel, C., Talon, S., Siess, L., 2006, A&A, 453, 261-278

Smiljanic, R., Gauderon, R., North, P., Barbuy, B., Charbonnel, C., Mowlavi, N, 2008, A&A, 502, 267-282

Smiljanic, R., Pasquini, L., Charbonnel C., Lagarde,N. , 2009, in press